Design and Development of a Multi-material, Cost-competitive, Lightweight Mid-size Sports Utility Vehicle's Body-in-White

Amit M. Deshpande[1, 2], Rushabh Sadiwala[3], Nathan Brown[3], Sai Aditya Pradeep[1], Leon M. Headings[6], Ningxiner Zhao[6], Brad Losey[6], Ryan Hahnlen[5], Marcelo J. Dapino[6], Gang Li [1, 3], Srikanth Pilla[1, 2, 3, 4]*

[1]Clemson Composites Center, Clemson University, Greenville, SC-29607
[2]Department of Automotive Engineering, Clemson University, Greenville, SC-29607
[3]Department of Mechanical Engineering, Clemson University, Clemson, SC-29634
[4]Department of Materials Science and Engineering, Clemson University, Clemson, SC-29634
[5]Strategic Research Operations, Honda Development & Manufacturing of America, LLC
[6]Department of Mechanical and Aerospace Engineering, The Ohio State University, Columbus, OH 43210

ABSTRACT

Vehicle light-weighting has allowed automotive original equipment manufacturers (OEMs) to improve fuel efficiency, incorporate value-adding features without a weight penalty, and extract better performance. The typical body-in-white (BiW) accounts for up to 40% of the total vehicle mass, making it the focus of light-weighting efforts through a) conceptual redesign b) design optimization using state-of-the-art computer-aided engineering (CAE) tools, and c) use of advanced high strength steels (AHSS), aluminum, magnesium, and/or fiber-reinforced plastic (FRP) composites. However, most of these light-weighting efforts have been focused on luxury/sports vehicles, with a relatively high price range and an average production of 100,000 units/year or less. With increasing sports utility vehicle (SUV) sales in North America, focus has shifted to developing lightweight designs for this segment. Thus, the U.S. Department of Energy's (DOE) Vehicle Technologies Office has initiated a multi-year research and development program to enable cost-effective light-weighting of a mid-size SUV. The proposed designs shall enable weight reduction of a minimum of 160 lb. (~72.7 kg), with a maximum allowable cost increase of $5 for every pound of weight reduced. The proposed designs shall enable vehicle production rates of 200,000 units/year and will be aimed at retaining the joining/assembly line employed by the OEM. A systems approach has been utilized to develop a multi-material, light-weight redesign of the SUV BiW that meets or exceeds the baseline structural performance. This study delves into the development of design targets for the proposed redesign at the system, sub-assembly, and component levels. Furthermore, results from topology optimization studies on a design volume were assessed to understand the load paths under various loading conditions. Several multi-material concept designs were proposed based on the insights provided by the topology optimization study. Novel multi-material joining methodologies have been incorporated to enable maximum retention of the OEM's joining and assembly process without significantly increasing cost. This paper presents the systems approach, and results from design studies undertaken to meet the program challenges.

*Keywords: Composites, Multi-material optimization, topology optimization, body-in-white, carbon fiber

*Corresponding author: spilla@clemson.edu; Ph: 864-283-7216

1. INTRODUCTION

Transportation accounted for 26.9 % of all energy consumption in the U.S.[1], and resulted in nearly 1/3rd of all CO_2 emissions[2]. Recent global energy markets and supply chain disruptions have given impetus to improve efficiency of transport systems. In the case of personal transportation, there has been a push

towards not only promoting efficient internal combustion engine vehicles (ICEVs), hybrid electric vehicles (HEVs), and battery electric vehicles (BEVs) but also developing cost-effective light-weighting solutions that utilize sustainable materials. The fact that a 10 % reduction in vehicle weight results in a 6-8 % improvement in fuel economy [3] has motivated key stakeholders to investigate light-weighting using light-weight materials such as aluminum, magnesium, and fiber-reinforced polymer (FRP) composites. These materials have the potential to reduce the weight of a vehicle's chassis or body-in-white (BiW) by up to 50 %[3]. This can also help compensate for the added weight of large and heavy battery systems for HEVs and BEVs, further improving the energy efficiency by working in tandem with efficient electrified powertrains. Ultimately, these gains can result in a cost benefit of up to $4.5 per kg of weight reduced over the product lifetime[4], [5]. Furthermore, it is estimated that for every kilogram of weight reduction, 20 kg CO_2 emissions reduction is achievable[6]. Traditional automotive BiW light-weighting approaches can be classified into three broad categories – a) design optimization [7] and associated manufacturing process development, b) material substitution[8] and c) conceptual redesign [9].

Table 1: Cost and weight reduction implications for light-weighting materials and approaches

Automotive Case Studies: Light-weighting Methodology			Light-weighting Materials*	Weight reduction Potential (%)	Specific Tensile Strength (MPa.m^3.kg^{-1})	Relative cost increment (multiplier)[5]
Design Optimization	Material Substitution	Conceptual Redesign				
[10]			Ductile Cast Iron	40 %	0.0063 [11]	1
[12]	[12]		HSS / AHSS	15-25 %	0.1481[13]	1 – 1.5
[14]	[14]	[15], [16]	Aluminum	40 %	0.1061[17]	1.3 – 2
[18][19]	[18][19]	[18][19]	Titanium	30-55 %	0.20[20]	1.5 – 10 +
	[21]	[22]	Magnesium	60-75 %	0.214[23]	1.5 – 2.5
[24]	[25]	[26]	Glass Fiber Composites**	25-35 %	0.59[17]	1 – 1.5
[9], [27]	[14], [15], [17]	[14], [15], [17]	Carbon Fiber Composites**	50-60 %	0.938[17]	2+
*It is assumed that the baseline component subject to light-weighting is made of mild steel as it is the most used material in BiWs[28] **Considers high strength epoxy and continuous unidirectional (UD) fiber preforms						

Table 1 highlights how most light-weighting approaches that leverage a single material system do not present a cost-effective solution, and conceptual redesigning and optimization to suit the light-weight material system often result in trade-offs in cost, increased manufacturing complexity and higher cycle times. This, inhibits the adoption of the new design concepts on a broader scale in the automotive industry, adding further to the cost, which would otherwise have gradually reduced with wider adoption in the industry. Thus, a multi-material light-weighting approach, capitalizing on the progress made in multiple material categories, is necessary to enable cost-effective light-weighting suitable for large-scale production. Table 2 summarizes some of the more prominent multi-material redesigns for the BiW that have been investigated for scaled production in the automotive industry.

Table 2: Multi-material BiW light-weighting designs

Ref.	Description	Composite Material Systems	Production Scale*	Product details – segment and vehicle model		Light-weighting potential **	Part Reduction ***	Cost Increment (multiplier)
[29]	Reinforcing BIW joints and cavities with composites and heat-activated structural adhesives, compatible with E-coat process	Thermoplastics	Small to Medium-Scale	Sports sedans, sedans	2019 Porsche Carrera Cabriolet B-pillar, 2006 Citroën C4 Picasso	75 %#	NA	1 - 2

[9]	Thermoset CRRP occupant cell, thermoplastic exterior panels, and aluminum sub-frame	Thermosets and Thermoplastics	Small-scale	Compact, sports coupes /sedans	BMW i3 and i8	25 %	66 %	NA
[9]	Multi-material design with selective use of CFRP composites	Thermosets	Medium scale	Luxury sedans	BMW 7 series	10-12 %	NA	1
[30]	Steel-CFRP-Aluminum hybrid construction with CFRP predominantly used for floor panels and side frame	Thermosets	Large-scale prototype	Compact car	Changan Eado ET	30 %	55 %	NA
[31]	Steel-CFRP-Aluminum monocoque-frame hybrid construction	Thermoplastics	Large-scale	sedan	Prototype (partnership with Japanese OEMs)	30 %	NA	1
[32]	CFRP-steel bonded structure for the roof to meet FMVSS 216 while achieving light-weighting	Thermosets	Large-scale prototype	Sedan /hatch-back	Toyota Yaris	68 % (max)	NA	NA
[33]	Modular multi-material design with structural occupant cell and semi-structural front and rear end assemblies with structural epoxy adhesives being used predominantly	Thermoplastics	Small-scale prototype	Compact car	Nido EV concept car	28 %	NA	NA
[15]	Comprehensive vehicle light-weighting using multi-material designs	Thermosets	Large-scale prototype	Sedan	MMLV Mach 2 program	45 %	NA	NA

*Small-scale production <50,000/year, Medium-scale production < 150,000/year, Large-scale production > 150,000/year

**Compared to equivalent steel reinforcements/ components

***Compared to equivalent steel intensive baseline design

#Indicates achievable light-weighting at a sub-assembly or component level

Despite the North American market exhibiting an increasing trend in the sales of SUVs and trucks, no previous studies specifically address their light-weighting through a systemic multi-material redesign utilizing FRP composites for the BiW. The case studies summarized in Table 2 focus on adhesive bonding and/or mechanical fastening/interlocking as the predominant multi-material joining method, requiring significant overhaul of the existing BiW joining and assembly infrastructure utilized by current automotive OEMs, making them incompatible with the scale and cost targets established for this project. In this study, the BiW of the 2019 Honda Pilot, a high-volume production, mid-size SUV for the North American market was selected. Hybrid metal-composite designs were considered highly feasible and were proposed considering the cost, joining, assembly and light-weighting targets set forth for the program.

2. APPROACH

The DOE project objectives (stated in the Abstract section) clearly define the scope for light-weighting and additional incurred costs to achieve said light-weighting. Furthermore, the design should meet all the packaging requirements and meet or exceed the structural performance requirements. These requirements have been established through benchmarking of the baseline BiW by performing structural analyses for several load cases. The overall technical approach follows the automotive industry's standard practice of product development based on the V-diagram[34]. Furthermore, because manufacturing processes play a very significant role in the end properties achieved, multiple simulation–validation loops have been incorporated into the approach at the coupon level, sub-component level, and assembly level. The approach is as illustrated in Figure 1. The subsequent sections elaborate on the efforts made on the design and simulation fronts to develop feasible multi-material light-weighting concepts for the baseline steel-intensive BiW of the 2019 Honda Pilot, which is as illustrated in Figure 2.
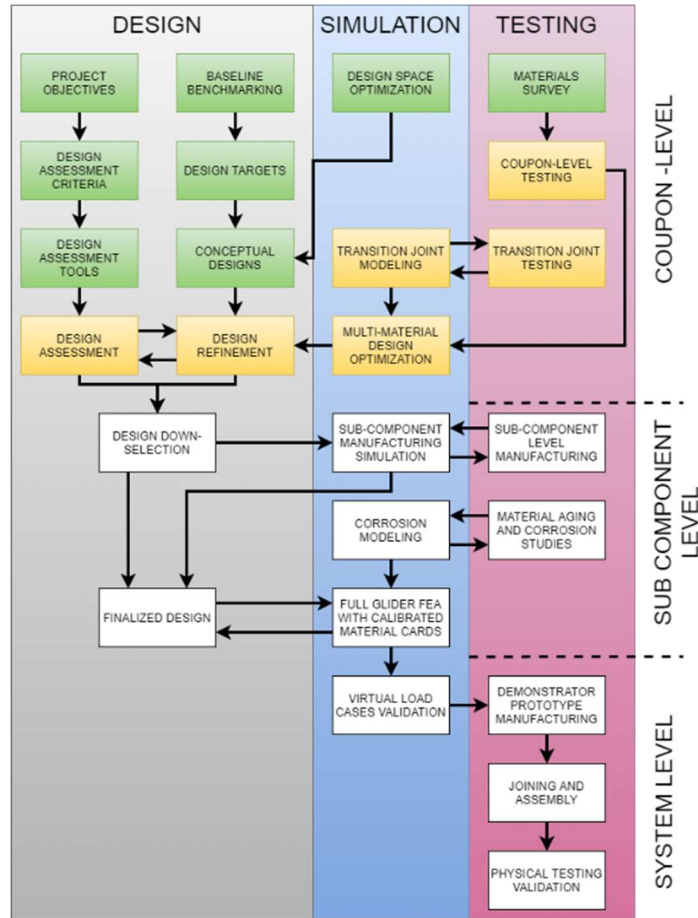
Figure 1: Overall Technical Approach

3. BASELINE BENCHMARKING

3.1. Design Benchmarking

The first step in developing new design concepts was to perform detailed benchmarking of the baseline. Parts serving as vital structural components were identified by studying the baseline performance under various load cases in conjunction with the OEM's recommendations. Small components such as local reinforcing plates, brackets and fasteners were identified as potential components that could be eliminated through parts consolidation. The glider assembly was divided into seven distinct sub-assemblies to be individually evaluated for different conceptual designs. The number of parts and weight were assessed for each of the sub-assemblies for use as a benchmark to compare the light-weighting and parts consolidation achievable in the proposed designs. The seven sub-assemblies are as illustrated as illustrated in Figure 2.
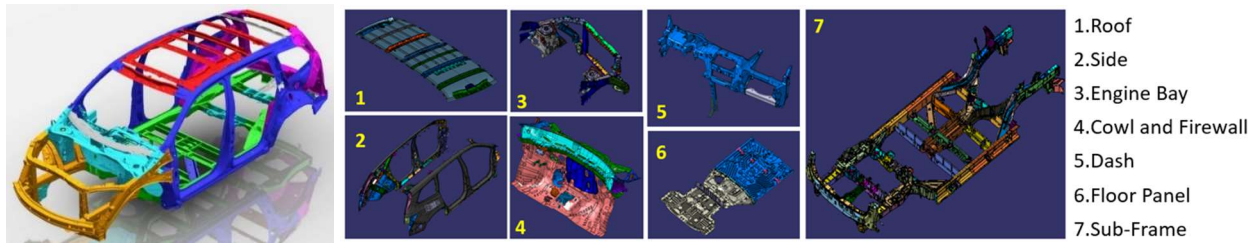
Figure 2: The Honda Pilot BiW (left) (Source: Honda America) categorized into sub-assemblies (right)

The parts and weights associated with the sub-assemblies were used to identify focus areas for light-weighting and parts consolidation using composites. The rationale behind this approach was that the cost of more expensive composite materials would be offset by less parts to be manufactured and assembled. This helped the design team identify conceptual designs that do not result in an overwhelming increase in the cost and assembly complexity; while also ensuring that the OEM's joining, and assembly infrastructure is still useful. The break-up of weight and number of parts according to the sub-assemblies is as illustrated in Figure 3.
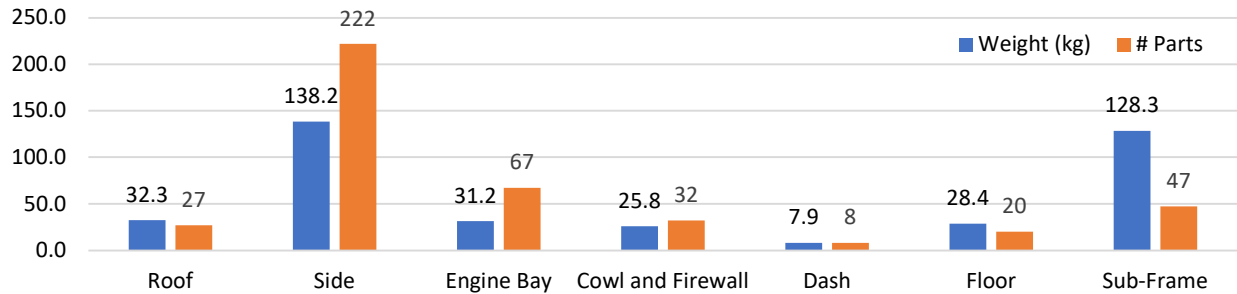
Figure 3: Weight and parts breakdown for key sub-assemblies of the baseline glider

3.2. Design Requirements

Per US DOE project goals, the light-weight glider must have zero compromises in its mechanical performance compared to the baseline 2019 Honda Pilot BiW. To achieve this, several static global load cases were considered and analyzed by the team at Clemson, as summarized in Table 3 and Figure 4.

Table 3: Global load cases for baseline glider structural performance benchmarking

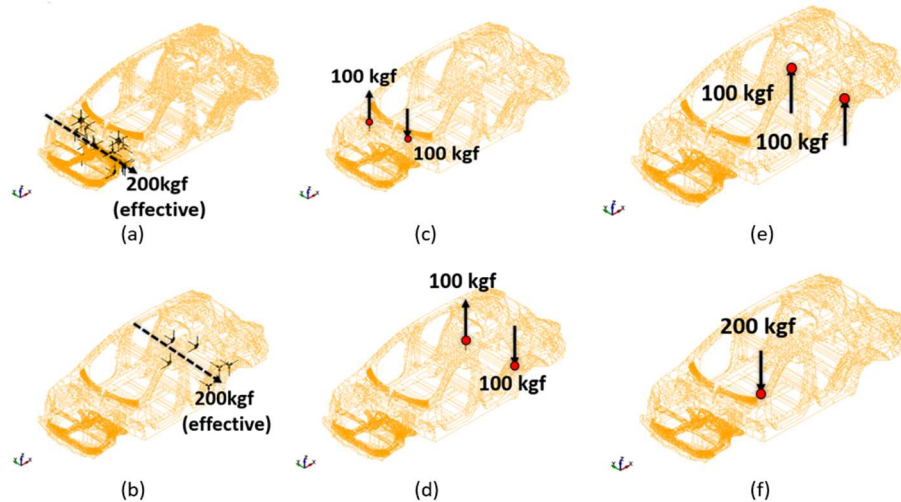| Load Case	Load Case Description
Front/Rear Lateral	simulates glider performance when a lateral force is applied at the front/rear suspension points.
Front/Rear Twist	quantifies the torsional rigidity when a twisting force is applied at the front/rear strut mounting points
Rear bending	quantifies the flexural rigidity when a bending force is applied at the rear struct mounting points.
Driver H-point Load	quantifies the flexural rigidity as a bending force is applied at the driver seat mounting points.

Figure 4: Description of load cases (a) Front Lateral (b) Rear Lateral (c) Front Twist (d) Rear Twist (e) Rear Bending (f) H-point [##]

5

The load cases were simulated by the project team at Clemson in a commercial finite element solver by Altair called Optistruct. The static load cases are solved as a linear static elasticity problem and the analysis is performed in conjunction with the inertia relief method in place of traditional boundary conditions. The displacement results for each load case are shown in Figure 5. Regions in red are locations with high displacements, whereas regions in blue represent low or negligible displacements. The direction of displacements at the load points has also been illustrated. High stress regions for each load case are shown in Figure 6 in red.
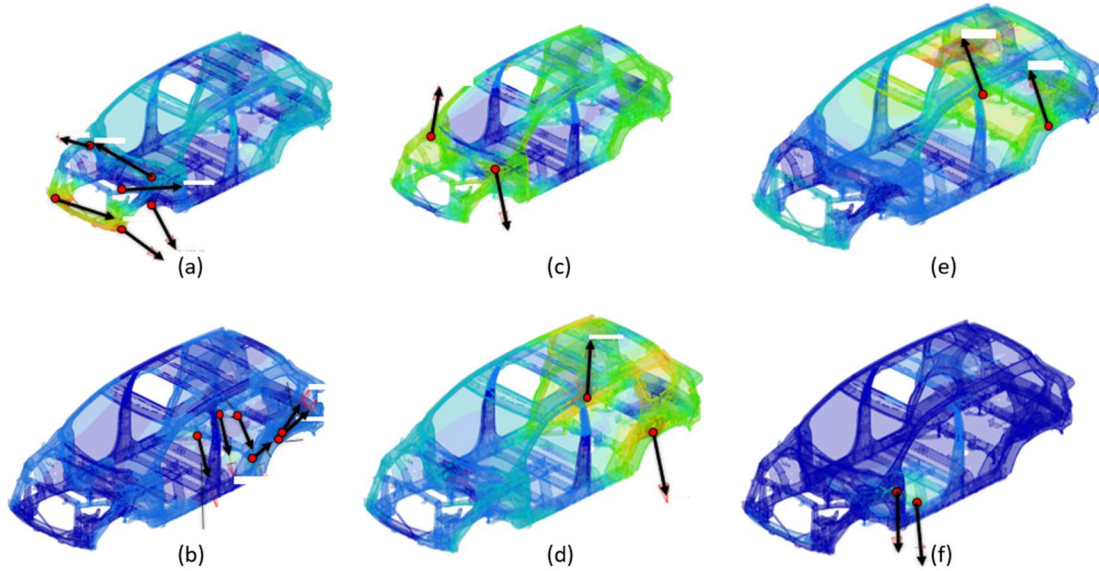
Figure 5: Displacement contour plots and load point displacements: (a) Front Lateral (b) Rear Lateral (c) Front Twist (d) Rear Twist (e) Rear Bending (f) H-point[##]
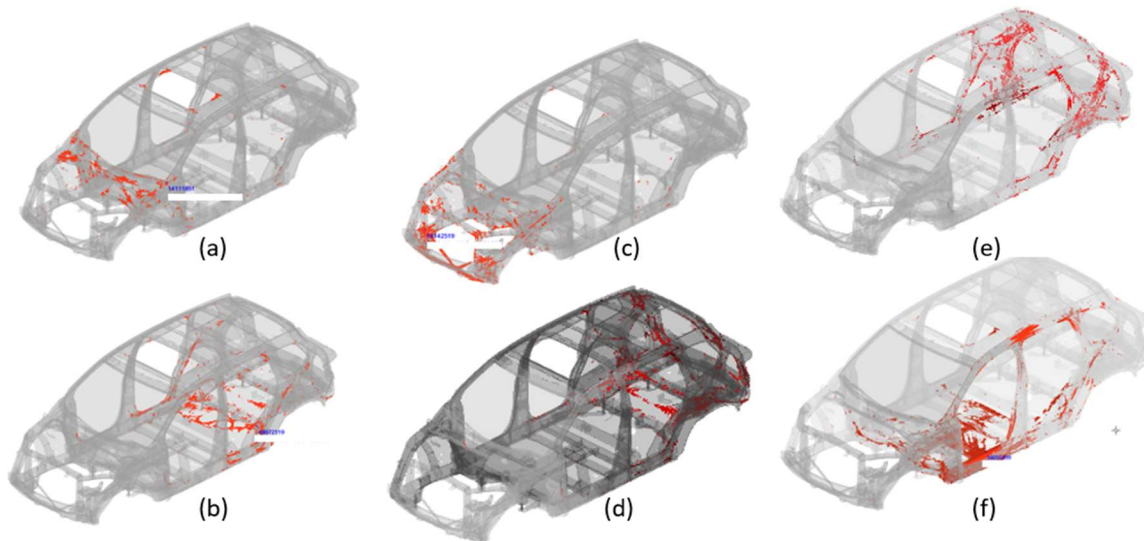

Figure 6: High-stress regions (a) Front Lateral (b) Rear Lateral (c) Front Twist (d) Rear Twist (e) Rear Bending (f) H-point[##]

Lastly, the stiffness of the glider against all load cases is calculated to quantify the response of the glider into one quantity independent of the scale of loads applied. It is calculated as the weighted sum of the ratio of forces to displacements at the load points.

$$K_i = \sum_{n=1}^{} w_n * \frac{F_n}{d_n}$$

[Eqn. 1]

Where, i indicates the load case, n indicates the load point, w is the weight provided by our OEM partner, F is the forces applied to the load point *'n'* and d is the displacement response at load point *'n'*. These stiffness values are further used as the design requirements, and hence used as constraints for the topology optimization problem.

3.3. Multi-material manufacturing and joining considerations

The next step was establishing a list of manufacturing processes and joining processes that could be leveraged in conceptual designs. This would define a conceptual design space that would be explored to come up with coherent design concepts. Inputs from the OEM were considered to identify processes that would fit their infrastructure and would, thus, be suitable from a cost and manufacturability standpoint. They have been summarized in Figure 7. The transition joint (TJ) occupies a central position among the different joining methods reviewed, since it is material agnostic and enables joining of weldable metals to the edges of lightweight FRP composite parts. This has been discussed in detail in section 3.4.
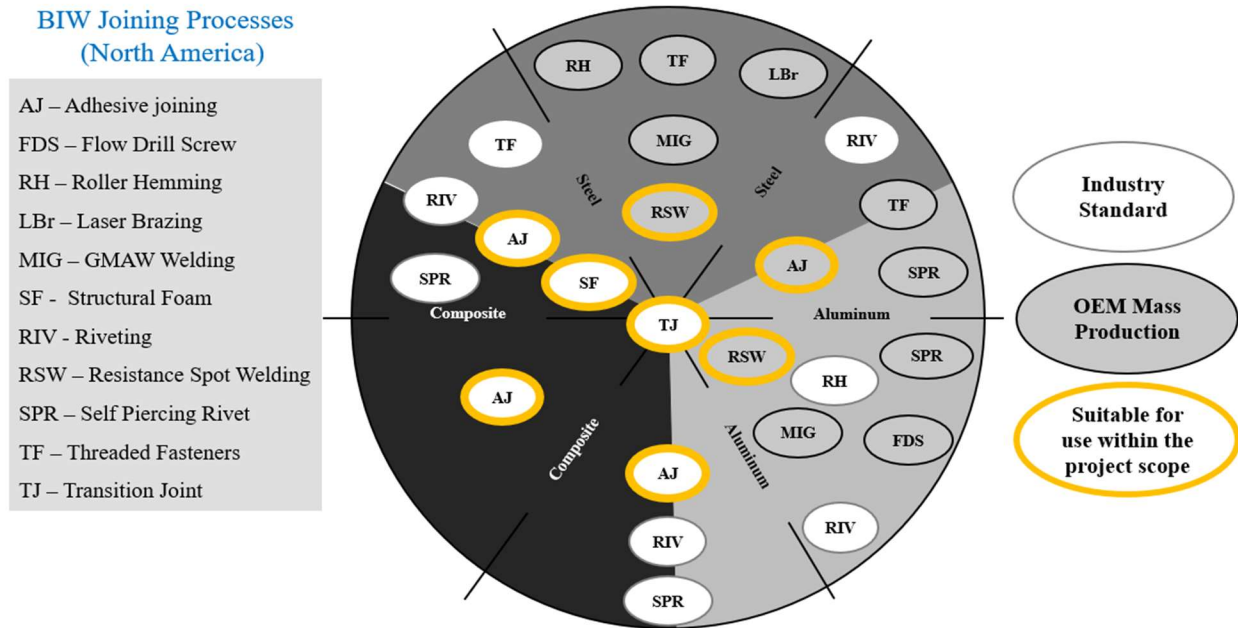

Figure 7: Joining processes reviewed for potential use with OEM's existing infrastructure

3.4. The Ultrasonic Additive Manufacturing (UAM) Process

Ultrasonic additive manufacturing (UAM) utilizes principles of solid-state ultrasonic metal welding to create metal parts using foil feedstock. A sonotrode is used to apply ultrasonic transverse vibrations (at a nominal frequency of 20 kHz) and a normal force (~5000 N) on the metal foil, leading to plastic deformation between the substrate and the new foil. The normal force and localized plastic deformation can displace surface oxides and contaminants while collapsing asperities, thus triggering the exposed nascent surfaces to form gapless metallurgical bonds, as illustrated in Figure 8. A computer numerical control (CNC) stage can selectively remove material and machine the parts to final dimensions. Repeated welding of foils in conjunction with sequential machining operations yields 3D-printed multi-material.
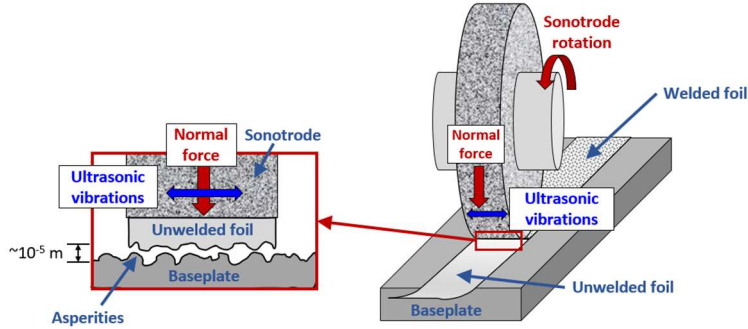
Figure 8: Schematic of UAM process[35]

Apart from welding dissimilar metals, UAM has also been demonstrated for joining high-strength fibers and metals. Transition joints of carbon fiber and aluminum alloy (AA) have been successfully built via UAM[35]. Dry carbon fibers (CF) are embedded into an AA matrix by placing fibers into channels machined in the metal matrix and welding metal foils or sheets overtop. The CF extending from the metal is then interleaved with additional CF plies and cured with epoxy to complete a lightweight CFRP-AA structure. This CFRP structure with AA tabs or flanges can be attached to a BiW structure using conventional joining methods such as resistance spot welding (RSW), as illustrated in Figure 9. The ability to produce CFRP-AA structures offline before being attached to the BiW like a conventional metal part enables CFRP integration in high-volume applications without slowing down the manufacturing process. The joint strength is obtained by mechanical interlocking of CF loops within the AA matrix; tensile tests demonstrate that the UAM welded joints have a strength of 129.5 MPa[35] and a specific energy absorption of 3.96 J at 0.8 mm displacement[35]. This process of producing metal-FRP transitions with UAM can be readily optimized and applied to various metal and fiber materials to suit different applications.
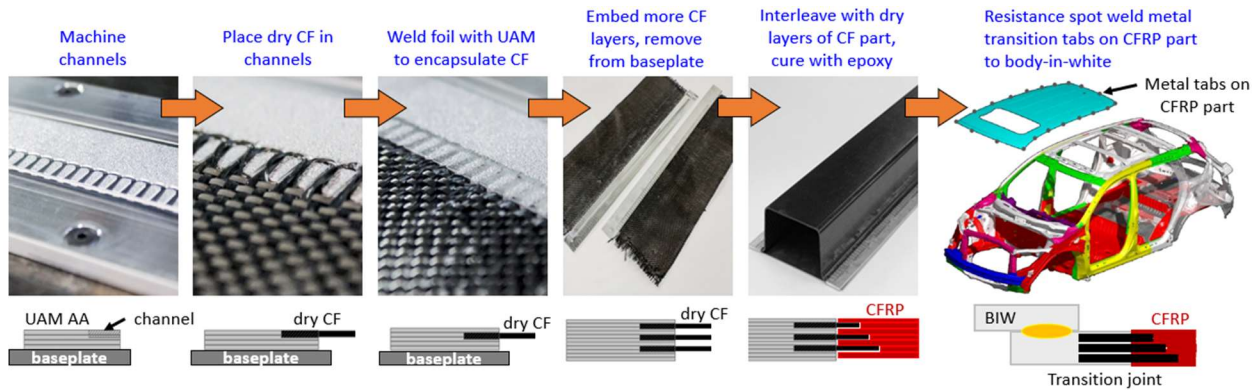

Figure 9: Adoption of the UAM process for CFRP-metal transition joints for use in automotive BiW

3.5. Topology Optimization Inputs

Topology optimization (TO) is a tool used for finding the optimal distribution of material against different load cases. For the initial topology optimization for the glider, it is assumed that the entire glider is made a single widely used material - steel. The OEM partner provided the allowable design space. The topology optimization process is described in Figure 10(left). The topology optimization problem is formulated as:

$$Min\ V$$
$$ST: \ \sigma < \sigma_{max}; \ K_i \geq K_i^{bl}$$

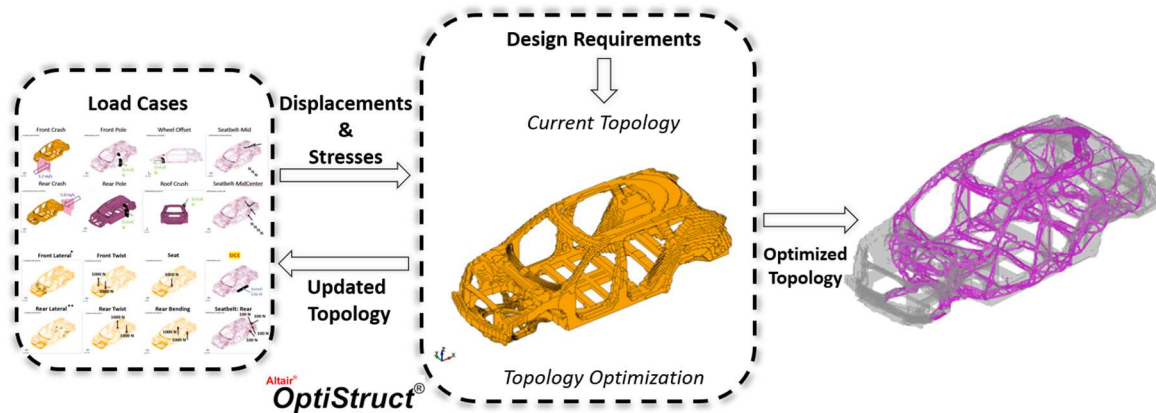Figure 10: Topology Optimization workflow and Single Material Topology Optimization result

Where V is the volume fraction of the current topology, σ is the stress at any point in the glider and σ_{max} is the maximum allowable stress. K_i indicates the current stiffness for the ith load case, and K_i^{bl} indicates the baseline stiffness for the ith load case. A minimum feature-length of 3mm is assumed. The topology optimization is performed on a commercial optimization package by Altair called OptiStruct. The optimized topology of the glider is shown in Figure 10(right). The optimized topology represents a design with the same mechanical characteristics (for the selected load cases) as the baseline glider, while achieving a 22.7 % weight reduction (compared to the baseline). These results are incomplete, as they currently do not factor in dynamic load cases such as crash cases. These results are used to visualize the load paths for all load cases, showing what parts are essential to resist those forces. This information will be used to down-select design concepts discussed in section 4.

4. DESIGN CONCEPTUALIZATION RESULTS

Following the benchmarking study and review of feasible manufacturing and joining processes, brainstorming was initiated to develop conceptual designs that would align with the project objectives. The overall approach to design conceptualization is as summarized in Figure 11. While conceptualizing designs, certain assumptions were made to estimate and compare the light-weighting potential and parts consolidation potential. It was assumed that any baseline steel component replaced with an equivalent composite or aluminum part would have twice the thickness of the baseline steel component. The initial light-weighting estimates were then calculated based on commonly available densities for typical aluminum and CFRP material with a thermoset epoxy matrix. Five design concepts were proposed and reviewed in detail, during a team-wide design brainstorming and assessment meet where industry experts from the OEM provided their valuable feedback. The conceptual designs have been summarized in
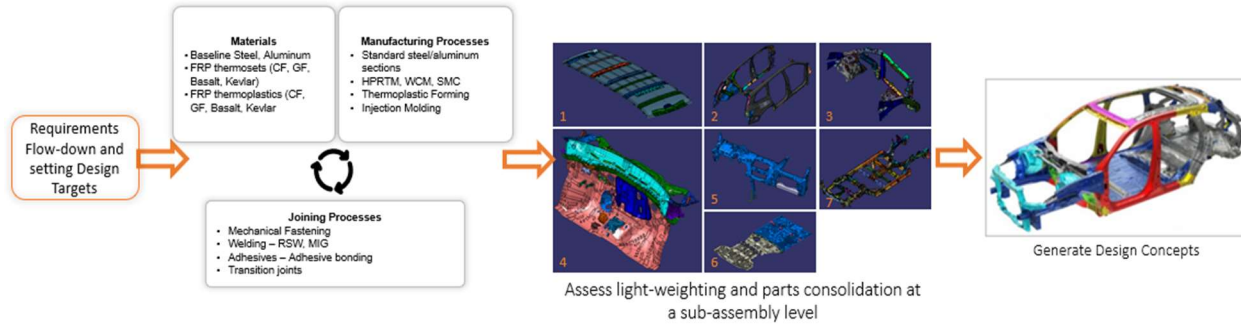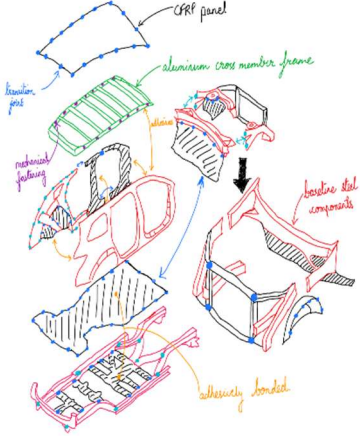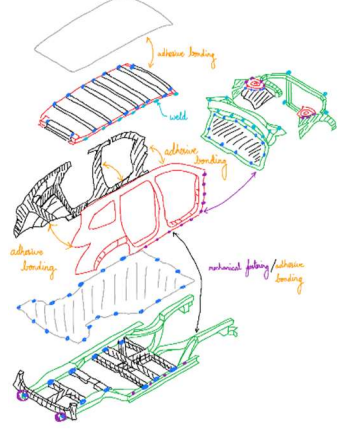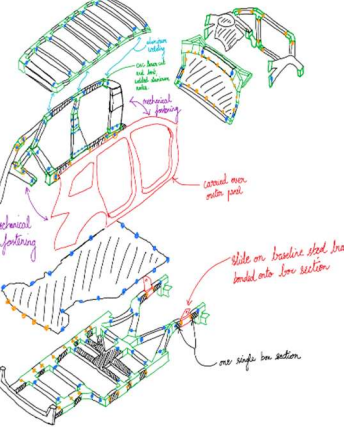Table 4 and Table 5.

Figure 11: Design conceptualization approach

Table 4: Conceptual designs' summary A

Concept 1	Concept 2
• Selective parts consolidation and light-weighting using composites. • Sub-frame redesigned as welded picture frame using standard aluminum sections with floor panel and cross-members being consolidated and made from composites. • Side sub-assembly redesigned with two inner reinforcing composite stiffeners running along the pillars • Transition joints enabling welds with adjacent sub-assemblies.	• Selective parts consolidation and light-weighting using composites. • The roof, floor, inner side stiffeners and the cross members of the sub-frame to be consolidated and subject to light-weighting. • Adhesive bonding and resistance spot welding enabled by the metal-CF transition joint were the only joining methods proposed for use in this concept.
• Weight Reduction Potential: 17.4 % (70.9 kg/156.5 lb. max. weight reduction possible)	• Weight Reduction Potential: 27 % (110.5 kg/243.7 lb. max weight reduction possible)
• Parts Consolidation Potential: 21.75 %	• Parts Consolidation Potential: 32.8 %
• OEM Assembly line compatibility: LOW	• OEM Assembly line compatibility: HIGH

Table 5: Conceptual designs' summary B

Concept 3	Concept 4	Concept 5

• Roof: Replacement of steel cross members • CFRP-steel construction with transition joints • Subframe outer members and mid-rails retained, cross members and floor consolidated into a composite design	• Welded Aluminum sections as frames for composite panels • use of basalt fibers/GFRP for panels • Side panel and stiffener sub-assembly consolidated into single composite design	• Spaceframe with metal nodes • Adhesive bonding • RSW + transition joints leveraged • Favorable for prototype technology demonstrator glider
• Weight Reduction Potential: 30 % 124.9 kg /275 lb. max. weight reduction possible	• Weight Reduction Potential: 43% 176.25 kg /388 lb. max. weight reduction possible	• Weight Reduction Potential: 39% 162.8 kg /358.9 lb. max. weight reduction possible
• Parts Consolidation Potential: 30.5 %	• Parts Consolidation Potential: 39.5 %	• Parts Consolidation Potential: 41 %
• OEM Assembly line compatibility: MODERATE	• OEM Assembly line compatibility: MODERATE to LOW	• OEM Assembly line compatibility: LOW

5. CONCLUSION AND FUTURE WORK

5.1. Conclusion

This study showcases a first in employing a holistic systems approach to conceptualize feasible multi-material light-weighting design concepts for the BiW of a large-scale production SUV. It effectively utilizes the knowledge gained from a detailed benchmarking study which included static structural performance evaluation for several load cases, and topology optimization performed on suitable design space representing the BiW. Five unique design concepts were proposed which leverage state-of-the-art large-scale composites manufacturing processes and transition joints that allow multi-material joining using existing joining processes. They were assessed for their scope offered in terms of weight reduction, parts consolidation, and compatibility with OEM's existing assembly line. They are currently being assessed and refined to meet the requirements of the OEM BiW joining and assembly line, enabled by the novel UAM transition joints that enhance mechanical joining of metals and FRP composites.

5.2. Future Work

A key deliverable of this project is to develop designs that enable sustainable use of recycled carbon fiber. Thus, each proposed design concept shall be assessed for the scope it offers for incorporating recycled carbon fiber formats developed by the project partners without compromising function or performance. To ensure manufacturability and translation of developed technologies into a scaled production environment, the manufacturing cost and cycle time reduction for the multi-material designs shall also be evaluated. Each proposed design concept will be graded on a scale of 1 to 10 with appropriate weightage for design criteria. The resulting decision matrix will allow further down-selection and refinement of the design concepts.

Structural performance assessment of the initial design concepts is dependent on producing accurate simulations, that utilize material databases that capture material response in various scenarios. Therefore, a critical component of future work involves material testing of the aluminum, steel, and carbon fiber samples. The experimental results of testing these materials in tension, compression, shear, and bending will be used to produce a material database card that can be passed to the multi-material BiW simulations. Additional static and dynamic load cases (summarized in Table 6), will be considered in the design refinement. Dynamic load cases will be solved as an implicit dynamic problem.

Table 6: Additional glider Load Cases (LC) to be considered

Wheel Offset (Static)	simulates the intrusion of front driver side wheel into the wheel well.
Roof Crush (Static)	quantifies strength-to-weight ratio when the roof is subjected to a crushing force (FMVSS 216)
Front/Rear small overlap impact (Dynamic)	quantifies the flexural rigidity of the glider when a bending force is applied at the rear struct mounting points.
Side Pole Impact (Dynamic)	simulates vehicle impact by a rigid pole at 32 kmph at 75 degrees (FMVSS 214)
Moving deformable barrier side impact (Dynamic)	simulates driver-side impact by a deformable barrier. (IIHS Side impact crashworthiness evaluation)

These load conditions will be incorporated into the single material topology optimization. Once the final single material TO problem is set up, the model will be modified to incorporate CFRP parts to undergo multi-material topology optimization (MMTO) whose results will be used for refining the designs.

Material database cards will be produced for the main structural components and the multi-material transition joints that make mechanical interlocking of the metal and composite possible. Separate simulation models must be produced to capture the highly complex response of the transition joints. The models will be simulated using LS-Dyna (*Ansys,* Canonsburg, PA) to capture the interaction between the CFRP loops and UAM metal inserts. The UAM metal body can be modeled using a material card mimicking the response of experimental testing. However, the CFRP body requires a more complex material card that can capture the microscopic interaction of carbon fiber and epoxy. Additionally, the strength of the CFRP loops depends on the orientation of the individual fibers. To address this additional level of complexity, Digimat (*Hexagon,* Stockholm, Sweden*)* will be incorporated to simultaneously capture the microscopic interactions between the two entities and fiber orientation. Digimat will feed the material properties of the CFRP according to its fiber orientation into the LS-Dyna model.

The simulation models will be used to capture the response of the transition joints under tension, shear, and bending. The results of these simulations can be compiled to produce a highly accurate material card that captures the physical response of the metal-CF transition joints. This material card can be used in the multi-material simulations and topology optimization. The material card will eliminate the need to model the metal-CF transition joint and instead represent the joint as a simple solid block that behaves according to the material card and, therefore, captures the appropriate response with a significant reduction in computation cost. Finally, upon validation, this joint model can be used to test the response of various metal (aluminum, steel) and fiber (carbon fiber, Kevlar, basalt) alternatives without experimental testing.

Feasibility for the proposed materials and manufacturing processes and the scalability required to meet the project goal shall be assessed. A plant layout aimed at retaining the OEM's existing assembly/joining process and infrastructure will be developed using Siemens Technomatix. The scope is limited to developing plant layouts for the joining and assembly of the glider sub-assemblies occurring on the OEM's factory floor, while processes such as the UAM transition joint fabrication and composite preform fabrication are excluded from the plant layout and cycle time assessment. Figure 12(a) illustrates a hypothetical fabrication process flow for different components of the glider. A high-level assembly process of these sub-assemblies to the glider at the OEM is shown in Figure 12(b).
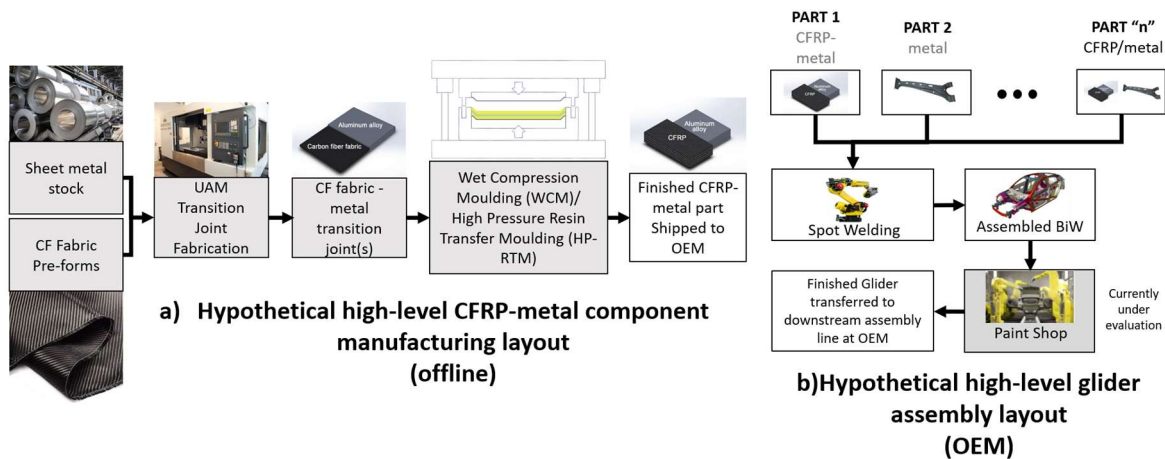
Figure 12: (a) Offline manufacturing of a CFRP-metal part; (b) Joining and assembly at OEM

This assembly process layout shall be incorporated in the cost model to assess the cost feasibility and obtain a cost value for the proposed design that can then be compared with the baseline's cost. Contrary to cycle time assessment and plant layout development, cost modeling shall incorporate major offline processes as well, such as fabrication of the cutting of composite fiber preforms, transition joints and manufacturing of composite parts. In addition to a survey of potential material costs, the cost and energy metrics associated with the patented transition joint fabrication process are also being studied. Once a preliminary plant layout is developed, a cost model will be developed that includes the cost of material, equipment, manufacturing/assembly labor, and energy consumed for the fabrication the glider.

6. ACKNOWLEDGEMENTS

7. DISCLAIMER

##Analysis and findings do not represent the standard development procedure followed by Honda for production vehicles.

8. REFERENCES

[1]   "Flowcharts." https://flowcharts.llnl.gov/ (accessed May 09, 2022).

[2]   "Carbon Flow Charts | Flowcharts." https://flowcharts.llnl.gov/commodities/carbon (accessed May 09, 2022).

[3]   "Lightweight Materials for Cars and Trucks | Department of Energy." https://www.energy.gov/eere/vehicles/lightweight-materials-cars-and-trucks (accessed May 09, 2022).

[4]   "Materials Research to Meet 21st-Century Defense Needs," Washington D.C., 2003. doi: 10.17226/10631.

[5]   A. Taub, E. de Moor, A. Luo, D. K. Matlock, J. G. Speer, and U. Vaidya, "Materials for Automotive Lightweighting," 2019, doi: 10.1146/annurev-matsci-070218.

[6]   B. P. Bhardwaj, *The Complete Book on Production of Automobile Components & Allied Products*. Delhi: NIIR Project Consultancy Services, 2014.

[7]   Xia L., *Multiscale Structural Topology Optimization*. London: Elsevier, 2016.

[8]   A. I. Taub, P. E. Krajewski, A. A. Luo, and J. N. Owens, "The evolution of technology for materials processing over the last 50 years: The automotive example," *JOM*, vol. 59, no. 2, pp. 48–57, 2007, doi: 10.1007/s11837-007-0022-7.

[9]   J. Starke, "CARBON COMPOSITES IN AUTOMOTIVE STRUCTURAL APPLICATIONS".

[10]   K. Fiedler, B. F. Rolfe, and T. de Souza, "Integrated Shape and Topology Optimization - Applications in automotive design and manufacturing," *SAE International Journal of Materials and Manufacturing*, vol. 10, no. 3, pp. 385–394, 2017, doi: 10.4271/2017-01-1344.

[11]   "Ductile Iron grade 65-45-12." https://www.matweb.com/search/datasheet.aspx?matguid=8ff2aecc7ac14df29b0cfc775e2d3726&ckck=1 (accessed May 13, 2022).

[12]   D. J. Andrea and W. R. Brown, "Material Selection Processes in the Automotive Industry Prepared for the Automotive Plastics Recycling Project," 1993.

[13]   "A New Global Formability Diagram - AHSS Guidelines." https://ahssinsights.org/blog/a-new-global-formability-diagram/ (accessed May 13, 2022).

[14]   J. Zhang, X. Zou, L. K. Yuan, and H. Zhang, "Lightweight Design of Automotive Front End Material-Structure Based on Frontal Collision," in *SAE Technical Papers*, Apr. 2020, vol. 2020-April, no. April. doi: 10.4271/2020-01-0204.

[15]   T. Skszek and J. Conklin, "Multi-Material Lightweight Vehicles," 2014.

[16]   "2020-battery-day-presentation-deck." https://tesla-share.thron.com/content/?id=96ea71cf-8fda-4648-a62c-753af436c3b6&pkey=S1dbei4 (accessed May 13, 2022).

[17]   A. K. Kaw, *Mechanics of composite materials*. Taylor & Francis, 2006.

[18]   M. Kuttolamadom, J. Jones, L. Mears, T. Kurfess, and K. Funk, "Life-Cycle Integration of Titanium Alloys into the Automotive Segment for Vehicle Light-Weighting: Part II - Component Life-Cycle Modeling and Cost Justification," *SAE International Journal of Materials and Manufacturing*, vol. 5, no. 1, pp. 260–269, 2012, doi: 10.4271/2012-01-0785.

[19]   S. Y. Sung and Y. J. Kim, "Economic net-shape forming of TiAl alloys for automotive parts," *Intermetallics (Barking)*, vol. 14, no. 10–11, pp. 1163–1167, Oct. 2006, doi: 10.1016/J.INTERMET.2005.11.025.

[20]   "Titanium Ti-6Al-4V (Grade 5), Annealed Bar." https://www.matweb.com/search/DataSheet.aspx?MatGUID=10d463eb3d3d4ff48fc57e0ad1037434&ckck=1 (accessed May 14, 2022).

[21]   M. K. Kulekci, "Magnesium and its alloys applications in automotive industry," *The International Journal of Advanced Manufacturing Technology 2007 39:9*, vol. 39, no. 9, pp. 851–865, Nov. 2007, doi: 10.1007/S00170-007-1279-2.

[22]   J. P. Weiler, "A review of magnesium die-castings for closure applications," *Journal of Magnesium and Alloys*, vol. 7, no. 2, pp. 297–304, Jun. 2019, doi: 10.1016/J.JMA.2019.02.005.

[23]   "Overview of materials for Magnesium Alloy." https://www.matweb.com/search/datasheet_print.aspx?matguid=4e6a4852b14c4b12998acf2f8316c07c (accessed May 14, 2022).

[24]   "Liz Nickels New innovations in automotive thermoplastics", doi: 10.1016/j.repl.2019.06.041.

[25]   V. Santhanakrishnan Balakrishnan, T. Hart-Rawung, J. Buhl, H. Seidlitz, and M. Bambach, "Impact and damage behaviour of FRP-metal hybrid laminates made by the reinforcement of glass fibers on 22MnB5 metal surface," *Composites Science and Technology*, vol. 187, p. 107949, Feb. 2020, doi: 10.1016/J.COMPSCITECH.2019.107949.

[26] S. Rajesh, G. B. Bhaskar, J. Venkatachalam, K. Pazhanivel, and S. Sagadevan, "Performance of leaf springs made of composite material subjected to low frequency impact loading †," *Journal of Mechanical Science and Technology*, vol. 30, no. 9, pp. 4291–4298, 2016, doi: 10.1007/s12206-016-0842-x.

[27] G. Gardiner, "Is the BMW 7 Series the future of autocomposites?," *Compositesworld*, 2016. https://www.compositesworld.com/articles/is-the-bmw-7-series-the-future-of-autocomposites (accessed May 13, 2022).

[28] P. Blain, "Steel Perspectives for the Automotive Industry," 2012. Accessed: May 13, 2022. [Online]. Available: https://www.oecd.org/industry/ind/50498824.pdf

[29] P. Malnati, "Composites as auto-body reinforcements," *Compositesworld*, 2021. https://www.compositesworld.com/articles/composites-as-auto-body-reinforcements (accessed May 13, 2022).

[30] "First Body-in-White Made from Composites for a Chinese Electric Car", Accessed: Jun. 05, 2022. [Online]. Available: www.springerprofessional.com/automotive

[31] J. Takahashi, "Strategies and Technological Challenges for Realizing Lightweight Mass Production Automobile by using Thermoplastic CFRP," 2011. Accessed: Jun. 27, 2022. [Online]. Available: http://j-t.o.oo7.jp/publications/20110820ppt.pdf

[32] M. R. Bambach, "Fibre composite strengthening of thin steel passenger vehicle roof structures," 2013, doi: 10.1016/j.tws.2013.09.018.

[33] E. Cischino *et al.*, "An Advanced Technological Lightweighted Solution for a Body in White," *Transportation Research Procedia*, vol. 14, pp. 1021–1030, Jan. 2016, doi: 10.1016/J.TRPRO.2016.05.082.

[34] "Using V-Diagrams in Engineering Projects — The Project Management Blueprint.com." https://www.theprojectmanagementblueprint.com/blog/procurements-management/the-v-diagram (accessed Jun. 21, 2022).

[35] H. Guo, M. B. Gingerich, L. M. Headings, R. Hahnlen, and M. J. Dapino, "Joining of carbon fiber and aluminum using ultrasonic additive manufacturing (UAM)," *Composite Structures*, vol. 208, pp. 180–188, Jan. 2019, doi: 10.1016/J.COMPSTRUCT.2018.10.004.

[36] A. Levy *et al.*, "Ultrasonic additive manufacturing of steel: Method, post-processing treatments and properties," *Journal of Materials Processing Technology*, vol. 256, pp. 183–189, Jun. 2018, doi: 10.1016/J.JMATPROTEC.2018.02.001.

[37] Z. Deng, M. B. Gingerich, T. Han, and M. J. Dapino, "Yttria-stabilized zirconia-aluminum matrix composites via ultrasonic additive manufacturing," *Composites Part B: Engineering*, vol. 151, pp. 215–221, Oct. 2018, doi: 10.1016/J.COMPOSITESB.2018.06.001.

[38] N. Sridharan, P. Wolcott, M. Dapino, and S. S. Babu, "Microstructure and texture evolution in aluminum and commercially pure titanium dissimilar welds fabricated using ultrasonic additive manufacturing," *Scripta Materialia*, vol. 117, pp. 1–5, May 2016, doi: 10.1016/J.SCRIPTAMAT.2016.02.013.

[39] C. D. Hopkins, P. J. Wolcott, M. J. Dapino, A. G. Truog, S. S. Babu, and S. A. Fernandez, "Optimizing ultrasonic additive manufactured Al 3003 properties with statistical modeling," *Journal of Engineering Materials and Technology*, vol. 134, no. 1, Jan. 2012, doi: 10.1115/1.4005269/455733.

[40] P. J. Wolcott, A. Hehr, and M. J. Dapino, "Optimized welding parameters for Al 6061 ultrasonic additive manufactured structures," *Journal of Materials Research*, vol. 29, no. 17, pp. 2055–2065, Sep. 2014, doi: 10.1557/jmr.2014.139.

[41] A. Hehr and M. J. Dapino, "Interfacial shear strength estimates of NiTi–Al matrix composites fabricated via ultrasonic additive manufacturing," *Composites Part B: Engineering*, vol. 77, pp. 199–208, Aug. 2015, doi: 10.1016/J.COMPOSITESB.2015.03.005.

[42] T. Han, C. H. Kuo, N. Sridharan, L. M. Headings, S. S. Babu, and M. J. Dapino, "Effect of weld power and interfacial temperature on mechanical strength and microstructure of carbon steel 4130 fabricated by ultrasonic additive manufacturing," *Manufacturing Letters*, vol. 25, pp. 64–69, Aug. 2020, doi: 10.1016/J.MFGLET.2020.07.006.

[43] C.-H. Kuo, N. Sridharan, T. Han, M. J. Dapino, and S. S. Babu, "Science and Technology of Welding and Joining Ultrasonic additive manufacturing of 4130 steel using Ni interlayers Ultrasonic additive manufacturing of 4130 steel using Ni interlayers," *Science and Technology of welding and Joining*, vol. 24, no. 5, pp. 382–390, 2019, doi: 10.1080/13621718.2019.1607486.